Title

Impacts of Adding Photovoltaic Solar System On-Board to Internal Combustion Engine Vehicles Towards Meeting 2025 Fuel Economy CAFE Standards

Journal

SAE International Journal of Alternative Powertrains, 5(2)

ISSN

2167-4205

Authors

Abdelhamid, Mahmoud
Haque, Imtiaz
Pilla, Srikanth
et al.

Publication Date

2016-04-05

DOI

10.4271/2016-01-1165

Peer reviewed

2016-01-1165
Published 04/05/2016

doi:10.4271/2016-01-1165
saealtpow.saejournals.org

Impacts of Adding Photovoltaic Solar System On-Board to Internal Combustion Engine Vehicles Towards Meeting 2025 Fuel Economy CAFE Standards

Mahmoud Abdelhamid
University of California, Merced

Imtiaz Haque, Srikanth Pilla, Zoran S. Filipi, and Rajendra Singh
Clemson University

ABSTRACT

The challenge of meeting the Corporate Average Fuel Economy (CAFE) standards of 2025 has led to major developments in the transportation sector, among which is the attempt to utilize clean energy sources. To date, use of solar energy as an auxiliary source of on-board fuel has not been extensively investigated. This paper is the first study at undertaking a comprehensive analysis of using solar energy on-board by means of photovoltaic (PV) technologies to enhance automotive fuel economies, extend driving ranges, reduce greenhouse gas (GHG) emissions, and ensure better economic value of internal combustion engine (ICE) -based vehicles to meet CAFE standards though 2025. This paper details and compares various aspects of hybrid solar electric vehicles with conventional ICE vehicles. Different driving locations, vehicle sizes, various driving patterns and different cost scenarios are used in order to enhance the current understanding of the applicability and effectiveness of using on-board PV modules in individual automobiles and ensure an accurate representation of driving conditions in all U.S states at any time. These times and location-dependent results obtained over a year show an increase in the combined mile per gallon (MPG) at noon in the range of 2.9-9.5% for a vehicle similar to a Tesla S, and a significant increase in the range of 10.7-42.2% for lightweight and aerodynamic efficient vehicles. In addition, by adding on-board PVs to cover less than 50% of the projected horizontal surface area of a typical mid-size vehicle (e.g., Toyota Camry or Nissan Leaf), up to 50% of total daily miles traveled by an average U.S. person could be driven by solar energy. Also, the return on investment (ROI) of adding PVs on-board with ICE vehicle over its lifetime shows only negative values when the price of gasoline remains below $4.0 per gallon and the vehicle is driven in low-solar energy area (e.g., Boston, MA). The same ROI is more than 250% if the vehicle is driven in high-solar energy area (e.g., Arizona), even if the gasoline price remains low. For future price scenarios, this ROI is much higher - nearly 10 times the investment cost under some scenarios, with the assumption of an eventual decline in battery costs. With regard to environmental impacts, significant gasoline gallons savings (~500-3400) and CO2 emission reduction (~5.0 to 34.0 short tons) are achieved.

CITATION: Abdelhamid, M., Haque, I., Pilla, S., Filipi, Z. et al., "Impacts of Adding Photovoltaic Solar System On-Board to Internal Combustion Engine Vehicles Towards Meeting 2025 Fuel Economy CAFE Standards," *SAE Int. J. Alt. Power.* 5(2):2016, doi:10.4271/2016-01-1165.

INTRODUCTION

Environmental concerns, high energy demand in the transport sector, and strong government regulations for 2017-2025 passenger cars and light trucks to reduce greenhouse gas (GHG) emissions and improve Corporate Average Fuel Economy (CAFE) standards [1] have led to increased focus on creating sustainable transportation technologies, not the least of which is the utilization of clean energy sources. U.S. Department of Energy, national labs, automotive OEMs, and academic researchers have been engaged in developing many solutions and models (e.g., ADVISOR model, PSAT, FASTSim, VISION, and GREET Model) to predict vehicle performance, emissions, and cost of alternative Powertrain technologies with different energy paths.

All above-mentioned efforts have overlooked the investigation of solar energy as an auxiliary on-board fuel. Widespread use of solar energy- a free, sustainable, renewable, and clean energy source - in fuel-efficient automobiles can ensure energy independence for U.S. while minimizing environmental impacts. Solar PV remains a promising technology for managing the on-board power systems of hybrid electric vehicles (HEVs). Technological advances in solar PVs have brought about efficiency improvements and cost reduction, and are expected to accelerate their inclusion in the automotive design process [2]-[4].

Although configurations exist for including on-board PVs in vehicles [5]-[9], current understanding on the efficacy of adding on-board PV technologies to internal combustion engines (ICE) for different vehicle sizes in different U.S locations under various driving scenarios remains incomplete. This paper is the first attempt at undertaking a comprehensive analysis of using solar energy on-board by means of PV technologies to enhance automotive fuel economies to meet CAFE standards though 2025 and extending driving ranges for ICE vehicles. In addition, in this paper we also estimate the economic

return on investment (ROI) and environmental impacts of adding on-board PVs to ICE vehicles under different scenarios. The proposed assessment methodology includes three different travel patterns in different U.S. states, covering different cost analysis scenarios for current and future prices.

MODELING ON-BOARD PV SYSTEM FOR ICE VEHICLES

Geographical Location

Total incident solar radiation (in kWh/m^2) for a specific period is known as global horizontal solar irradiation (G or GHI). GHI has two components: DNI and DHI. DNI, or direct normal irradiance, represents the solar energy that reaches the ground directly (in a straight line) from the sun, while DHI, or diffused horizontal irradiance, is derived from either scattering or diffusion of molecules and particles in the atmosphere. As the annual GHI in U.S. varies from state to state (see Figure 1 [10]), two cities which represent the extremities in terms of available solar energy were selected; (i) Phoenix, AZ and (ii) Boston, MA.

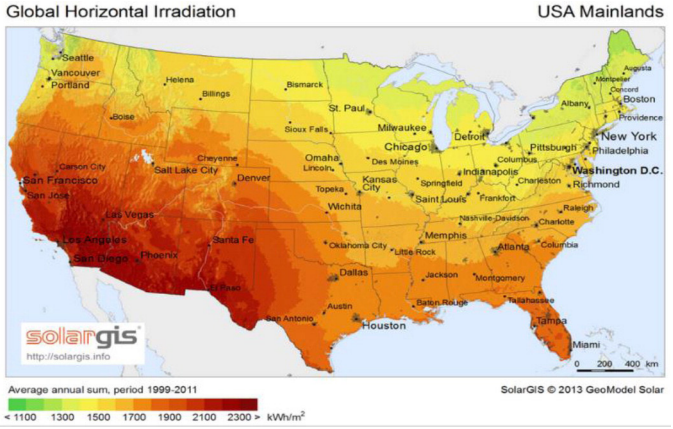

Figure 1. Annually global horizontal irradiation (G) in U.S. states [10]

PV Device

PV module is a packaged assembly of individual PV cells. A solar PV cell is an electronic device (p-n junction) that converts electromagnetic radiation near the visible range into direct electric current (DC). Previously, we developed two novel knowledge-based systems to evaluate and select the optimum solar PV module type for on-board vehicle applications [7], [8]. Mono-crystalline silicon (mono-Si) PV type was selected as the current best commercial option. The equivalent PV cell (module) circuit is modeled as shown in Figure 2 - consisting of a current source, a parallel diode, a series resistance (R_s), and a parallel (shunt) resistance (R_p). Four-parameter approach is used for modeling, which means that R_p is assumed to be infinite and is hence ignored. Current (I) and voltage (V) are calculated using Equations (1), (2), (3), (4) [11], [12]. The current generated by incident light (I_{pv}) depends on sun irradiation. R_s reflects the internal resistance, while R_p is typically due to manufacturing defects [13], [14].

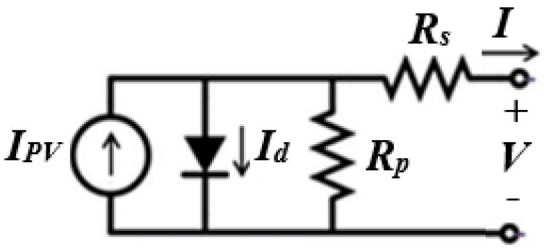

Figure 2. PV device equivalent circuit

$$I = I_{PV} - I_d - \frac{V + R_S.I}{R_p} \tag{1}$$

$$I_{PV}(T) = \frac{G}{G(nom)}\left[I_{SC}(T_{1,nom}) + \left(\frac{I_{SC}(T_2) - I_{SC}(T_1)}{(T_2 - T_1)}\right).(T - T_1)\right] \tag{2}$$

$$I_d = I_0\left(e^{\frac{q(V+I.R_S)}{nkT}} - 1\right) \tag{3}$$

$$I_0 = \frac{I_{SC}(T_1)}{\left(e^{\frac{q.V_{OC}(T_1)}{nkT_1}} - 1\right)} \times \left(\frac{T}{T_1}\right)^{\frac{3}{n}} \times e^{\frac{q.V_q(T_1)}{nk\left(\frac{1}{T} - \frac{1}{T_1}\right)}} \tag{4}$$

A transcendental Equation (5), which does not have a direct solution, is generated by substituting Equations (2), (3), (4) in Equation (1).

$$I - f(G, T, V_g, n, R_s, R_{Sh}, I, V) = 0 \tag{5}$$

Parameters I_L and I_o are calculated. V_g is set to 1.12, a typical value for crystalline silicon PV module. Other parameters (n and R_s) are estimated using curve-fitting approach, where the values of these parameters are tuned, with the objective function being to minimize the maximum PV module power to be within the accuracy range of the reported peak power of the PV module manufacturer data. Highly efficient mono-Si PV module, developed by the Sunpower Company [15], is used to validate the results of the proposed model by comparing the actual manufacturers' data and the predicted model results, as shown in Figure 3. Solid lines represent the actual I-V curves reported by manufacturers, while the "triangle and circle" are the results of this proposed model. All the curves at 25ºC unless otherwise is indicated.

In this work, an incremental conductance algorithm [16] is implemented in order to track the maximum power points, implying the optimal voltage and current that the PV system needs to work. Opting for a mounted structure of PV solar module on the vehicle surface affects both temperature (T) and the PV module performance. An empirically based thermal model [17] is used to estimate the thermal performance of PV. The optimum configuration of the PV module is observed to be the open rack: glass/cell/glass configuration.

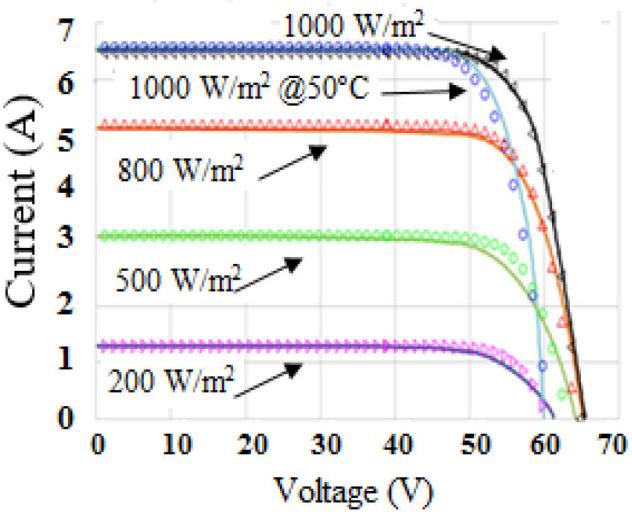

Figure 3. I-V Curves of PV module: Actual data (solid lines) vs. model results (circles/triangles)

Shadow and Sky Clearness

DNI that reaches the PV module is affected by shadows, while, DHI component is affected by the clearness of the sky. The solar data used here is the typical daily solar irradiance data that's collected by the National Renewable Energy Laboratory (NREL) / National Solar Radiation Data Base (NSRDB. It is called Typical Meteorological Year 3 and measured on an hourly base over 30 years based on empirical radiation data collected by meteorological station and include local weather variation which can dramatically change the radiation intensity [18].

Equations (6) and (7) are used to calculate GHI in both parking (p) and driving (d) modes.

$$\mathrm{GHI}_{\mathrm{Parking\,Mode}} = \alpha_P \times \mathrm{DNI} \times \cos(\theta) + \Psi_p \times \mathrm{DHI} \tag{6}$$

$$\mathrm{GHI}_{\mathrm{Driving\,Mode}} = \alpha_d \times \mathrm{DNI} \times \cos(\theta) + \Psi_d \times \mathrm{DHI} \tag{7}$$

Where α and ψ are the shadow factor and sky clearness factor respectively. The α factor is vary between 0 and 1 and changes with time and depend on weather, surroundings, and locations. While, ψ is already included in the collected DHI values.

PV Position

GHI reaches on-board PV module depending on the tilt and azimuth angles of PV installation. In general, for both fixed ground mounted and roof-top PV applications, the optimum tilt angle is around the latitude of the geographical location, with the PV face (azimuth angle) to the south or north direction. For on-board PV use in vehicle applications, the module can face any direction in both parking and driving modes. Our results show that in such case, the optimum tilt angle is horizontal when PV module is fixed; this also eliminates any problems that may arise due to aerodynamics. However, if the PV module(s) are placed on a curved vehicle surface, different PV cells (or modules) will have different angles of incidence (θ) with respect to the sun, and I will be different for each module. If these modules are connected in series, some of them must work with I not equal to I_{mp}. Consequently, net I for the PV module series will be the lowest I value, and a power mismatch problem will occur. DNI depends on (θ), and the power mismatch between the modules will be related to the difference between these different angles of incidence.

Two PV modules placed on a curved vehicle surface are shown in Figure 4. Angles of incidence of the PV modules 1 and 2 are θ_1 and θ_2 respectively. Power mismatch between the two modules is calculated using Equation (8). Assume that the curvature of the vehicle surface between the two regions where the two PV modules are installed, introduces a difference in incidence angles of less than 10°. If the sun is perpendicular to module 1 ($\theta_1 = 0°$), power mismatch losses will be minor (~ < 1.52%). However, if $\theta_1 = 50°$ (i.e. It is significant), then the power mismatch loss is around 14.3% (i.e. Power mismatch loss is also significant). Ideally, both the PV modules should be as parallel as possible.

$$\mathrm{Missmatchloss} = \left|\cos(\theta_1 \cdot \pi/180) - \cos(\theta_2 \cdot \pi/180)\right| \times 100\% \tag{8}$$

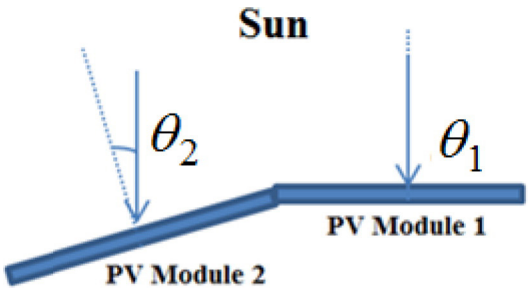

Figure 4. Angling PV on Vehicle Surface

Energy Storage and Vehicle Energy at Wheels

Energy demand at the wheels (E_W) for a given driving cycle and given vehicle, assuming the road grade to be zero, is calculated using Equation (9).

$$E_W = \frac{1}{2}.\rho_a.C_d.A_f.\int_{Cycle} v^3 dt + M_v.g.C_r.\int_{Cycle} v\ dt + 1.1.M_v.\int_{Cycle} V\frac{dV}{dt} \tag{9}$$

Energy generated by the PV module is stored using Li-ion polymer battery, about which full specifications and analysis are detailed elsewhere [19]. The slightly higher expected voltage of the PV module permits the use of the more efficient step-down DC-DC configuration. Equations (10), (11), (12) are used to calculate the solar energy-to-battery charging efficiency [20]. Charging efficiency is optimized when PV voltage is slightly higher than battery voltage. Optimum ratio V_{mp} to the battery voltage is equal to 1.029 and provides the best charging efficiency.

$$\mathrm{Eff}\,(\%) = \left(\frac{\mathrm{Avg.Voltage}\,(V) \times \mathrm{Charge\,Increase}(Ah)}{\mathrm{Avg.Solar\,Irrad.}\,(W/m^2) \times \mathrm{PV\,Area}\,(m^2)} \times \frac{\mathrm{Battery\,Charg.Eff.}\,(\%)}{\mathrm{Time\ Interval}(hr)}\right) \tag{10}$$

$$\text{Charge Increase} = \textit{Current} \times \text{Time} \tag{11}$$

$$\eta = \frac{\int_{I<0} (E_0 . I) dt}{\int_{I<0} (V . I) dt} \tag{12}$$

Total energy stored (in kWh) for varying time and varying PV installation areas in the battery at Phoenix, AZ is shown in Figure 5. Here, approximately 0.421 kWh of stored energy is available in the battery at noon with a PV installation area of 2.5 m^2 and solar efficiency at STC that is equal to 20%. Total estimated energy stored in the battery using an assumed PV module (area =3.26 m^2) represents the daily energy generation equal to 4.81 kWh in June in Phoenix, AZ and 1.036 kWh in December in Boston, MA (see Appendix Table 1 for estimation of stored energy at different times).

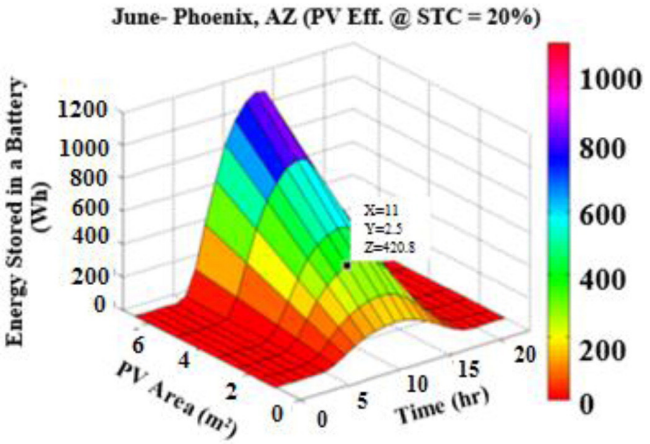

Figure 5. Energy stored in battery in June in Phoenix, AZ

RELATION OF CAFE STANDARDS WITH PV INSTALLATION SURFACE AREA

CAFE target, based on the vehicle footprint and PV output, depends on the installation area - typically the vehicle surface. We present in detail how we correlate the projected vehicle surface area with the 2020 and 2025 CAFE standards to determine the PV installation area required for these CAFE targets. Eight 2014-model vehicles with varying sizes are used: i) a two-seater car (Smart Fortwo), ii) a mini-compact car (Fiat 500e), iii) two sub-compact cars (Chevrolet Spark EV and Mitsubishi i-MiEV), iv) a compact size vehicle (Ford Focus), v) a mid-size vehicle (Nissan Leaf), vi) a large-size vehicle (Tesla Motor S), and vii) a small station wagon (Honda Fit). CAFE standard curves up to 2025 for passenger cars are provided in Figure 6 [1]. While x-axis represents the vehicle footprint in square feet (ft^2), vehicle footprint is defined as the area consisting of the vehicle's wheelbase multiplied by the average track width.

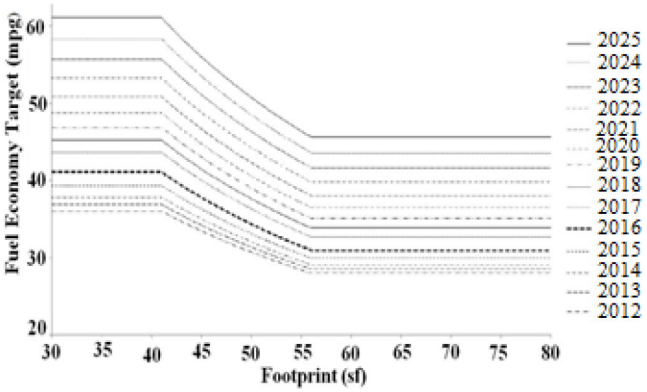

Figure 6. CAFE (MPG) Standard Curves for Passenger Cars [1], edited for clearness

CAFE target (MPG) curves for years 2020 and 2025 can be re-written as a criterion (13).

ft / MPG	$CAFE$ 2020	$CAFE$ 2025
$ft \le 3.8m^2$	49	61
$3.8m^2 < ft < 5.1m^2$	$-0.93.ft^2 + 87.07$	$-1.07.ft^2 + 104.93$
$ft \ge 5.1m^2$	36	46

(13)

Where ft is in square feet. .

Correlation between the reported values of vehicles' footprints and the projected horizontal surface areas of the eight selected vehicles is shown in Figure 7. Projected horizontal surface area for each vehicle is calculated based on the length and the width of the concerned vehicle. The predicted relationship (Equation 14) shows a linear relationship with R^2 equal to 0.9637, which is too high.

$$\text{Predicted Projected Horizontal Area} = 2.28 \times ft - 1.56 \tag{14}$$

Where, ft and predicted projected horizontal area are in square meters (m^2).

The maximum error between the actual and predicted values of projected horizontal surface areas is found in the case of I-MiEV and Ford Focus vehicles - about 0.75 m^2 and 0.32 m^2 respectively - while for most other vehicles, the error is less than 0.1 m^2. The relation between the projected horizontal surface areas of vehicles and their CAFE targets in 2020 and 2025 is expressed using the criterion (15).

	CAFE in 2020	CAFE in 2025
$HS \le 7.1\,m^2$	49	61
$7.1\,m^2 < HS < 10\,m^2$	36 - 49	46 - 61
$HS \ge 10\,m^2$	36	46

(15)

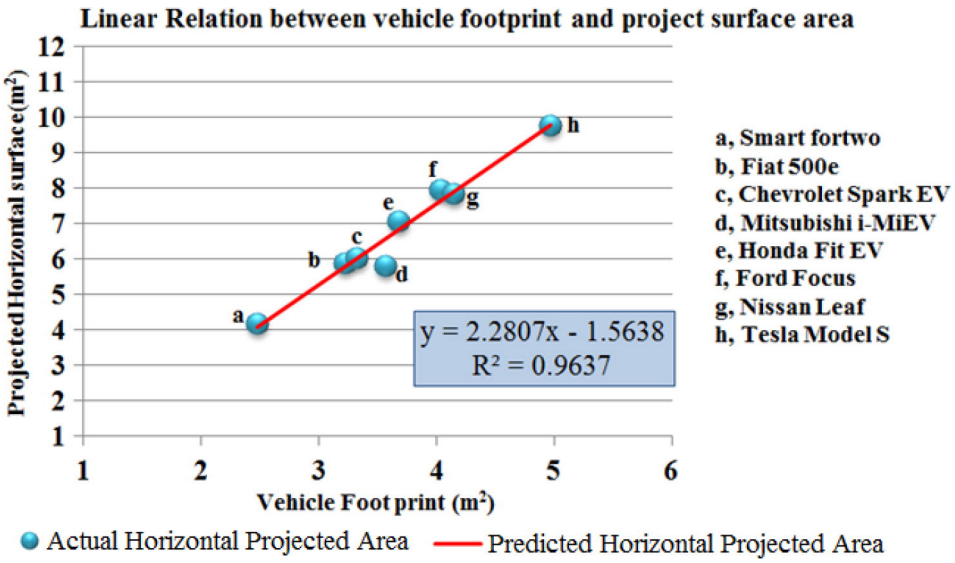

Figure 7. Predicted projected horizontal surface based on vehicle footprint for selected 2014 EVs

Consequently, for the highest CAFE target related to a vehicle footprint of less than 41 ft^2 (3.8 m^2) the horizontal projected surface (HS) area is less than 7.1 m^2. However, the vehicle design must be optimized to install PV modules on the entirety of this area for a typical vehicle, which is challenging. Since we have assumed only 50% of the projected horizontal surface area as being covered with PV modules, this turns out to be approximately 3.26 m^2, roughly the area of two assumed PV modules [15].

DRIVING PATTERN SCENARIOS

Most vehicles are rarely driven for long distances in the U.S., with the average daily vehicle trips approximately 36 miles with an average person trip length is 9.75 miles [21]. The percent (%) of person-trips by time of day (how frequent the U.S driver starts the trip by specific time) is shown in Figure 8 [21]. As can be seen, approximately 85% of all trips occur between 6 am and 7 pm, when solar energy is available. In this duration, three driving time scenarios are assumed: 9-10 am, 12 noon-1 pm, and 4-5 pm, since the highest percent of trips in a typical day occur during these times.

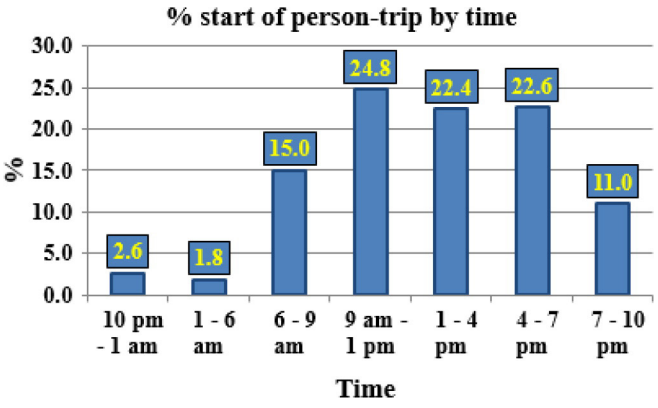

Figure 8. The percent of trips by day in the U.S [Data from [21]]

RESULTS AND DISCUSSION

Assumptions

Five vehicles with different sizes are analyzed (See Table 1). Key assumptions used in this analysis are tabulated in Table 2. Area of the PV base module is 1.63 m^2 (1.559 m x 1.046 m) [15], with the vehicle surface fitted with this PV module. Assumed installed PV area is 3.26 m^2, with the assumption of a constant width and a variable length with series connection to perform the required PV area (constrained by a constant PV efficiency). To ensure an accurate representation of driving conditions in all U.S states at any time, two scenarios are used: minimum values for the vehicle driven in Boston, MA in December; and maximum values for the vehicle driven in Phoenix, AZ in June.

Table 1. Different size assumed vehicles

Vehicle	Specification	Parameters similar to
Vehicle 1	C_d=0.17, A_f=1.2, C_r=0.008, and curb weight (M_v) =900 kg	Volkswagen XL1
Vehicle 2	(with C_d=0.17, A_f=1.2, C_r=0.008, and curb weight (M_v) =600 kg	Assumed very lightweight and aerodynamically very efficient
Vehicle 3	C_d= 0.29, A_f = 2.27, C_r=0.008, and curb weight (M_v) =1532 kg	Nissan Leaf 2012
Vehicle 4	C_d= 0.28, A_f = 2.25, C_r=0.008, and curb weight (M_v) =1447 kg	Toyota Camry 2014
Vehicle 5	C_d= 0.256, A_f = 2.36, C_r=0.008, and curb weight (M_v) =2110 kg	Tesla 2013 S

Table 2. Main assumptions

Description	Assumption
The usage of PV for vehicle	On-board
PV Types/Specifications	Mono-Si [15]
Area of PV installation	3.26 m^2
Shade factor	Factor =1 (Optimum case)
Mounting option	Open rack: glass/cell/polymer sheet
MPPT implemented	Yes
Tilt option	No
Tracking option	No
Energy Storage	Li-ion Battery (5 kWh)
Scenarios	Maximum related to June in Phoenix, AZ. Minimum related to December in Boston, MA
Vehicle lifetime	160,000 miles (GREET assumption [27])
Regeneration option	No (energy at the wheel is calculated for the worst case scenario)
Driving cycles	UDDS/ HWFET
Tank-to-Wheel Efficiency (η_{T2W})	ICE powertrain Efficiency = 15% at city cycle and 20% at highway cycle. For on-board PV 90%
Vehicle	Vehicle 1 to 5 (See Table 1)

Contribution of On-Board PV toward CAFE 2025

Fuel economy (FE) in terms of MPG in given driving cycles is calculated using Equation (16).

$$\mathrm{MPG} = \eta_{\mathrm{T2W}} \times \frac{E_{gasoline}}{E_{cycle}} \times I_{Cycle} \tag{16}$$

Where E_{gasoline} is the energy for a gallon of gasoline, assumed to be 33.7 kWh/gallon, I_{Cycle} is the cycle length, which depends on the driving cycle, E_{cycle} is the vehicle energy consumption depends on the vehicle parameters as well as driving cycle, and η_{T2W} is tank-to-wheel efficiency, based on Powertrain configurations and driving cycle. The combined fuel economy (FE) is calculated based on the city and the highway driving cycles using Equation (17). The weights of the city and highway driving cycles are considered as 55% and 45% respectively.

$$\mathrm{FE\,(combined)} = \frac{1}{\frac{0.55}{\mathrm{City\ FE}} + \frac{0.45}{\mathrm{Hwy\ FE}}} \tag{17}$$

η_{T2W} varies from low values as in the case of gasoline vehicles (typically 15-25%) to extremely high values as in the case of electric vehicles - for example, Tesla's electric Powertrain has an efficiency of 88%. Equations (18) and (19) are then used to calculate the contribution of on-board PV in increasing FE.

$$\mathrm{MPG_{City}} = \eta_{\mathrm{T2W_{city}}} \times \frac{E_{gasoline}}{(E_{citycycle} - E_{PV\,at\,wheel-citycycle})} \times I_{citycycle} \tag{18}$$

$$\mathrm{MPG_{Hwy}} = \eta_{\mathrm{T2W_{Hwy}}} \times \frac{E_{gasoline}}{(E_{\mathrm{Hwy}cycle} - E_{PV\,at\,wheel-\mathrm{Hwy}cycle})} \times I_{\mathrm{Hwy}cycle} \tag{19}$$

Where, $E_{\mathrm{PV\ at\ wheel\text{-}city\ cycle}}$ is the PV energy provided at the wheel in the duration of the city driving cycle, $E_{\mathrm{PV\ at\ the\ wheel\text{-}Hwy\ cycle}}$ is the PV energy provided at the wheel in the duration of the highway driving cycle, while $\eta_{\mathrm{T2W\_city}}$ and $\eta_{\mathrm{T2W\_Hwy}}$ are the tank-to-wheel efficiencies of the ICE conventional vehicle (prior to adding PV) in both city and highway cycles respectively. PV energy that reaches the wheels ($E_{\mathrm{PV\ at\ the\ wheel}}$) in a given driving cycle is calculated using Equation (20).

$$E_{PV\,at\,wheel} = T_{\mathrm{Cycle}} \times \eta_{PV2W} \times E_{PV-hourly} \tag{20}$$

Where, $E_{\mathrm{PV\_hourly}}$,is a PV hourly energy generation at a specific time and location (see Appendix Table 1), T_{cycle} is the cycle duration in hours (e.g., T_{cycle} = 0.38 in city cycle and 0.2125 in highway cycle), and η_{PV2W} is tank-to-wheel efficiency from PV module to wheels, assumed here as 90% (close to Tesla efficiency). Sophisticated estimation for η_{PV2W} requires further optimization for both the specific vehicle component size and the specific driving pattern. The idea here is to minimize energy conversion losses through the use of any available solar energy directly to the wheels without storing energy in the battery unless the system is forced to do so (e.g. SOC). However, such optimization depends on many parameters, specifically the size of the components, battery SOC, driving cycle, and control strategy [22].

Percentage (%) increase in combined MPG after adding the proposed PV on-board for different conventional gasoline vehicles at different times is illustrated in Figure 9. Five vehicle specifications covering a wide range of vehicles were analyzed (see Table 1). We calculated the combined fuel economy (mpg) prior to the addition of PV modules for all the above-mentioned vehicles, as shown in Figure 9 (x-axis) by assuming that all vehicles have a conventional internal combustion engine with $\eta_{\mathrm{T2W\_city}}$ = 15% and $\eta_{\mathrm{T2W\_Hwy}}$ = 20%. On the y-axis is plotted the minimum and maximum percentage increase in mpg for the three driving times: 9-10 am, 12 noon-1 pm, and 4-5 pm. The minimum and maximum values refer to the vehicles driven in Boston, MA in December, and in Phoenix, AZ in June respectively.

An increase in the combined MPG was found ranging between the minor value of 0.46% and the significantly higher value of 42.16%, with vehicle specifications, time, location, and month being the major determinants of the final mpg. For example, an increment in the combined mpg at noon for vehicle 4 (similar to Toyota Camry) ranged from 3.88% to 12.88%. Since the original combined mpg for vehicle 4 is 32 mpg, the minimum increase in its mpg after addition of PV is 1.24 mpg (3.88% x 32 mpg) if the vehicle is driven in December in Boston, MA while the maximum increment is 4.12 mpg (12.88% x 32 mpg) if the vehicle is driven in Phoenix, AZ in June.

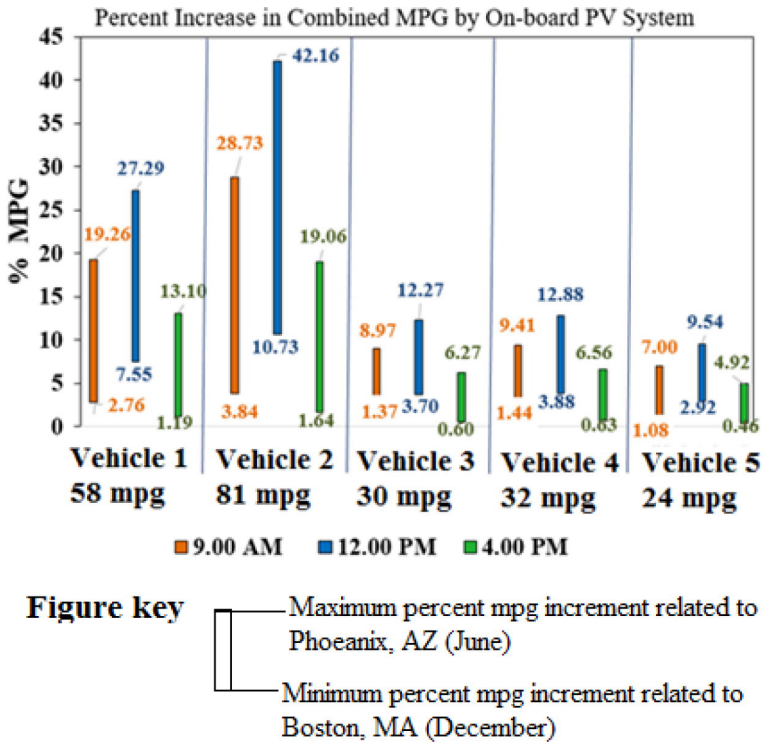

Figure 9. On-board PV contribution in the combined fuel economy (MPG) in different scenarios

As shown in Figure 9, the maximum PV contribution in vehicle 5 (similar to Tesla) is 9.54% of 24 mpg, equal to 2.29 mpg - because of the relative heaviest curb weight and cycle time, this is a relatively short value when compared to the total number of hours in a day when the sun is available. For vehicle 2, FE increased during the 4-5 pm driving time by 1.64% of 81 mpg, equal to 1.33 mpg in December in Boston, MA. A similar increase was seen in the 12 noon-1 pm driving time in Phoenix, AZ with an increase in FE to 34.15 mpg (42.16% of 81 mpg). For a typical mid-size car (Nissan Leaf or Toyota Camry), FE increased up to 4.2 MPG on using on-board PV system at noon.

PV SOLAR DAILY RANGE EXTENDER

The daily pure PV solar range extender is estimated for all assumed vehicles by adding the on-board PV system (see Figure 10). Efficiency (Wh/mile) for vehicles 1, 3, and 5 are calculated based on the reported EPA rated combined FE [23]. For non-electric vehicles 2 and 4, we estimated the driving ranges based on the optimized powertrain configuration η_{T2W} = 90% (as shown in y-axis, Figure 10). Extended daily driving ranges fell in the range of 3.0 to 62.5 miles as shown in Figure 10. For highly efficient vehicles (e.g., vehicle 2), the driving range is from 13.5 to 62.5 miles for any daily drive in any part of US. Results also indicate that of the total daily miles driven by a motorist in the US in a mid-size vehicle (vehicle 3 and 4), 50% could be powered via PVs. For a lightweight and aerodynamically efficient vehicle (vehicle 2), it is triple of the previous figure, up to 174%.

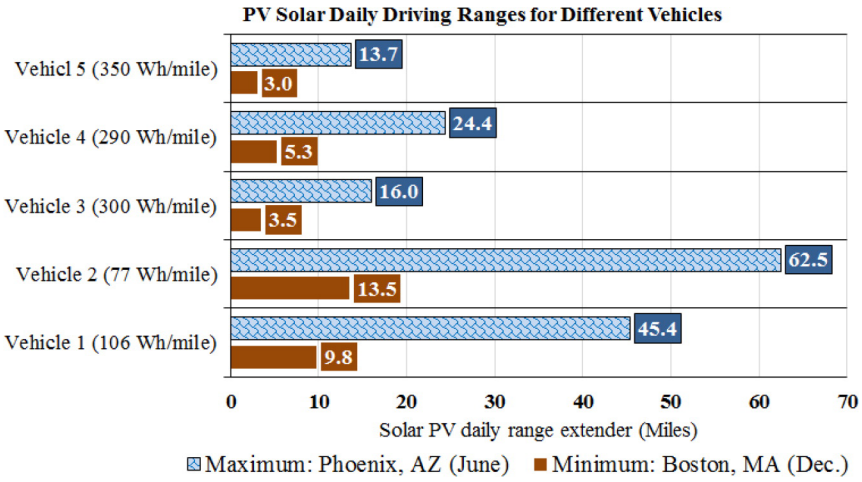

Figure 10. Solar PV daily range extender

RETURN ON INVESTMENT (ROI) OF HYBRID ICE VEHICLE WITH ON-BOARD PV SYSTEM

This section details the estimated rates of return on money (cost of adding on-board PV system) per period for an ICE vehicle, otherwise known as ROI, as expressed in Equation (21).

$$\mathrm{ROI}(\%) = \frac{\text{Gain of Investment} - \text{Cost of Investment}}{\text{Cost of Investment}} \times 100\% \quad (21)$$

Total cost of investment is calculated using Equation (22), which includes lifetime cost of the entire powertrain components. We used two cost scenarios (j) for market price - current and projected future. Assumptions and detailed calculations are found in Appendix (Table 2).

$$\text{Cost of Investment}(\$) = \sum_{j}[\text{PV module} + \text{Battery} + \text{Motor}] \quad (22)$$

Cost of the PV module is estimated based on both current and future prices [24]. Costs of battery and motor with controller were calculated using Equations (23) and (24), both of which are already in use in NREL Future Automotive Systems Technology Simulator [25].

$$\text{Motor and Controller}(\$) = \$21.7/\text{kW} + \$425 \quad (23)$$

$$\text{Battery}(\$) = \$22/\text{kW} + \$500/\text{kWh} + \$680 \quad (24)$$

Developments in battery technology have yielded a concurrent decline in price over the last few years. Priced at around $500/kWh in 2012, battery prices have fallen to $325/kWh in 2014, and are expected to decline further to $125/kWh by 2022 [26]. Equation (24) is modified to reflect these changes in costs, and the battery was also sized appropriately to accommodate energy demand in the maximum scenario. Equation (25) is used to calculate the gain on investment, specifically through analysis using three prices of a gallon of gas: $2.0, $4.0 and $8.0.

$$\text{Gain on Investment}_i = \frac{1}{\text{Vehicle MPG}} \times \text{PV Daily Solar Range} \times \text{Cost of Gasoline Gallon} \times 365 \times \text{Vehicle lifetime in Year}\ ] \quad (25)$$

The PV daily solar ranges are based on the minimum (i.e., driving in December in Boston, MA) and maximum scenarios (driving in June in Phoenix, AZ). Life of the vehicle was set at 12 years based on an average daily use of 36 miles, culminating in a total of 160,000 miles over the car's lifetime [21], [27]. Results for the three scenarios are shown in Figures 11, 12 and 13. When the price of a gallon of gas was $2.0 for current PV and battery prices (see Figure 11) and the car was driven in the low solar climate of Boston, MA, ROI had a negative value in the range -73.0 to -60.0%. When the price of a gallon of gas was $4.0 for current PV and battery prices (see Figure 12) and the car was driven in the low solar climate of Boston, MA, ROI had a negative value in the range -21.0 to -46.0%.

However, when the car was driven in the high solar climate of Phoenix, AZ with the same price for a gallon of gas, ROI was positive for the previous two scenarios and varied in the range 147%-263% (in case of scenario II), depending upon the vehicle specifications. For example, using the proposed on-board PV system with vehicle 4 (e.g. Toyota Camry) in Arizona, gain on investment was 2.5 times the investment cost. At gasoline price of $8.0/gallon and projected PV and battery prices (see Figure 13), in the low solar energy location of Boston, positive ROI was obtained, ranging between 62% and 135%. Naturally, this same ROI was more than 900% for the same vehicle operating in the sunny climate of Arizona. Although the lifetime of an average vehicle is approximately 12 years, lifetime of the PV module within those cars is more than 30 years. Our calculations are restricted to the vehicle lifetime, with the assumption being that these PV modules can be transferred to other applications after the vehicle is recycled. We intend to analyze this enhanced economic consideration in our future research.

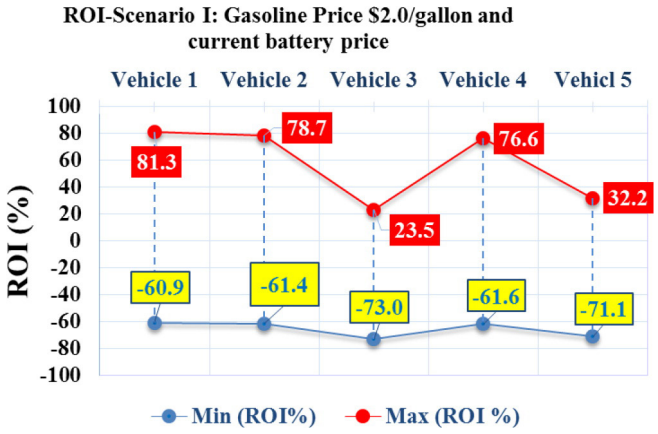

Figure 11. Minimum and maximum ROI of adding on-board PV for different ICE vehicles (Scenario I)

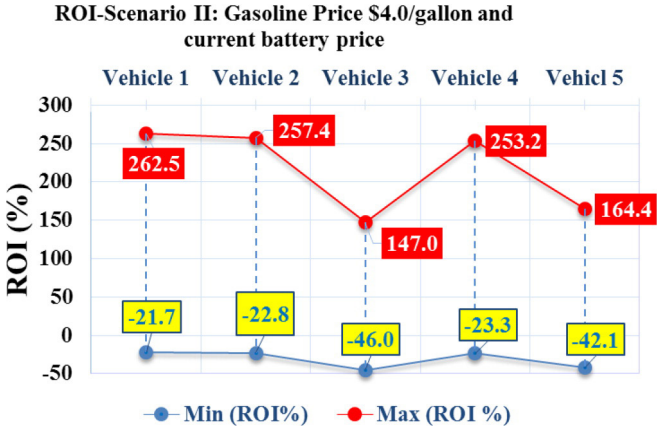

Figure 12. Minimum and maximum ROI of adding on-board PV for different ICE vehicles (Scenario II)

The economic considerations of the annual degradation of PV performance were not examined in this research. However, this is minor, the PV module efficiency is degraded linearly by 0.5% per year for the lifespan of 30 years. This mean based on the vehicle lifetime, the difference between the average efficiency of PV module consider this degradation compared to what used in this study is only 0.72%.

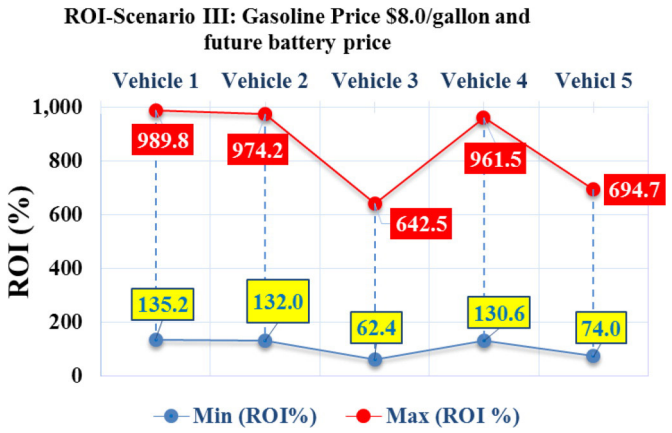

Figure 13. Minimum and maximum ROI of adding on-board PV for different ICE vehicles (Scenario III)

ENVIRONMENTAL IMPACT OF THE HYBRID ICE VEHICLE WITH ON-BOARD PV SYSTEM

Reduction in gasoline burning (see Figure 14) and carbon dioxide (CO_2) emissions (see Figure 15) by using hybrid solar vehicle in place of a conventional ICE vehicle over a 12-year life cycle was compared. Based on our calculations, a reduction of ~500 to 3400 gallons in gasoline use was obtained compared to a conventional ICE vehicle. Burning a single gallon of gasoline produces on an average around 19.64 pounds of CO_2, so over a 12-year life cycle for both cars, approximately ~ 5.0 to 34 U.S (short) tons of CO_2 reduction could be achieved by adding PVs with the ICE vehicles.

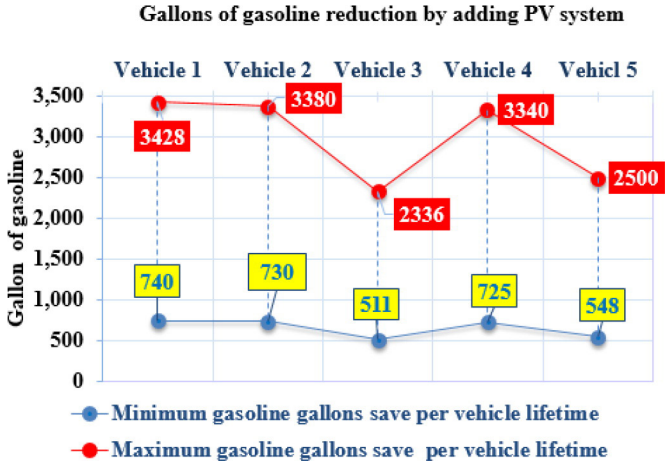

Figure 14. Minimum and maximum gallons of gasoline reduce per vehicle lifetime by adding on-board PV

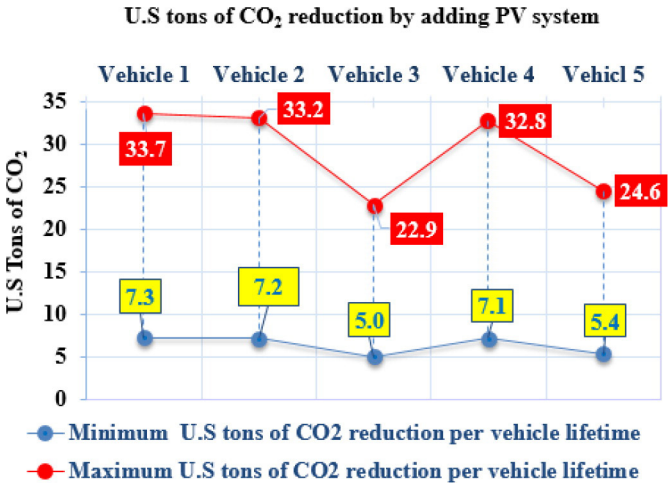

Figure 15. Minimum and maximum U.S. tons of CO_2 reduce per vehicle lifetime by adding on-board PV

EFFECTS OF MOUNTING ON-BOARD PV ON VEHICLE AERODYNAMICS

The preferred mounting option for PVs is the roof rack option compared to the insulated back option. However, the insulated back option may be preferred for aesthetic issues and will not affect the vehicle aerodynamics. The mono-Si PV module thickness is around 4.6 mm, which is very minor compared to the vehicle frontal area (2.0 m^2). The roof rack option resulted with a minor effect on the fuel economy by (1-3%) depending on vehicle parameters, e.g., added roof rack ~2% fuel economy for vehicle test with weight 1408 kg and the frontal area was 2.15 m^2 [28], [29], which means around 4 Wh energy consumption is increased per a mile, if the on-board PV module with roof rack option is installed in a vehicle with the original driving efficiency of 200 Wh/mile. However, future works are needed to test the aerodynamic impacts for specific targeted vehicles.

CHALLENGES OF VEHICLE DESIGN WITH ON-BOARD PV

Some of the previous discussions entailed optimizing solar power from the sun to the wheels via surface area, mounting, and orientation. Here, we detail concerns with the weight of the vehicle on incorporating onboard PVs in a conventional vehicle, specifically engine and battery mass scaling, both of which are based on Equations (26) and (27) respectively [30].

$$\text{Engine mass} = 0.47 \times \text{Engine Power} + 61 \quad (26)$$

$$\text{Li - ion Battery mass} = 8.5 \times \text{Batt. Energy} + 58 \quad (27)$$

Where engine mass and battery mass are represented in kilograms (kg), engine power is represented in kilowatts (kW), and battery energy is represented in kilowatt hours (kWh).

The electric motor is similar to that used in Stella solar vehicle [5]. Weight analysis from the addition of a PV module to a gasoline vehicle is shown in Appendix Table 3. Current scenario shows extra weight in the range of the 130.0 to 147 kg. The extra weight of Powertrain components should be balanced by light-weighting of some other components in the vehicle to keep the curb weight constant.

Comparing the weights of the real vehicles with solar race vehicles are still far away. For example, Eindhoven's solar powered car Stella weighs is only 380 kg [5], with energy consumption is around 40.2 Wh per mile.

CONCLUSIONS

Solar PV technology shows great promise for managing on-board power systems of HEVs and PHEVs. Widespread use of solar energy - a free, sustainable, renewable, and environmentally clean energy source - will help ensure energy independence for US while allowing the manufacture of fuel-efficient automobiles. This study presented a novel comprehensive assessment methodology regarding the use of PV solar technologies on-board with gasoline ICE vehicles to meet CAFE 2025 standards.

We uniquely related the 2020 and 2025 CAFE standard curves to the projected horizontal vehicle surface area for eight different vehicles of varying sizes in our study to estimate the maximum possible PV installation area for each CAFE target. We then determined the maximum contribution of on-board PV in enhancing fuel economy in the combined driving cycle for three travel patterns and five different vehicle sizes. The vehicle driven in December in Boston, MA was the minimal scenario while the maximum was the vehicle driven in June in Phoenix, AZ to determine the mean average for driving conditions in the other 48 U.S states at any time. A slight increase in the combined MPG (range 2.9-9.5%) at noon was observed for a vehicle similar to Tesla 2013 S while a significant increase in combined MPG (range 10.7-42.2%) was observed for lightweight and aerodynamic efficient vehicles. However, the short duration of the driving cycle - as little as 0.38 hours in the city cycle and 0.21 hours in the highway cycle - made comparing the hours in day of solar energy availability difficult.

Next, estimation of the pure PV solar range (PV range extender) for five different size vehicles was presented. It was determined that the addition of an on-board PV covered less than 50% (3.2 m^2) of the projected horizontal surface area of a typical vehicle. It was effective in extending the pure solar PV ranges to 50% of the total daily drive time of a U.S. mid-size vehicle. In addition, the combination of a lightweight and aerodynamically efficient vehicle with proposed PVs increased the total person miles of travel per day in the U.S. (using solar energy) by 174%. The daily driving range was observed to extend between 3.0 and 62.5 miles, based on vehicle specifications, locations, and time. For example, the addition of the proposed PV module to very lightweight and aerodynamically efficient vehicles could extend the daily range to between 13.5 miles and 62.5 miles. In the specific case of vehicle similar to Nissan Leaf, the range was extended - a minimum of 3.5 miles and a maximum of 16.0 miles. For a heavier vehicle similar to Tesla Model S 2013, a totally solar powered PV extended the driving range to between 3.0 and 13.7 miles.

When the vehicle was driven in a low solar energy location (e.g., Boston, MA) with the average price of a gallon of gas less than $4.0 and at today's PV and battery prices, ROI was negative. Under the same price in a high solar environment (e.g., Arizona), however, ROI was positive, varying between 147%-257%, depending upon on the vehicle specifications. If the price of a gallon of gas was $8.0 with the assumption of an eventual decline in battery costs, even in low solar energy locations a positive ROI was possible in the range of 60-135%, while ROI goes up to 1000% for vehicles in high solar energy locations. These results are based on an average 12-year life cycle of the vehicle. However, the life of the PV module extends well beyond this time by as much as 18 years, meaning that it can be transferred into another application after the vehicle is recycled. Economic considerations of this transfer though were not examined in this research. For an ICE vehicle with an assumed life-expectancy of 12 years and with an on-board PV system, estimates of gas savings ranged from a minimum of 500 to more than 3,400 gallons, with a concurrent reduction in nearly 5 to 33 U.S (short) metric tons of CO_2 emissions also reduced during that time.

The results of this dynamic model, which can reflect the various PV module areas, efficiencies, installation locations, times, and weather, are applicable for determining the on-board PV contribution for any vehicle size. Specifically, the proposed work can be used to develop a tool for decision-makers to use during the conceptual design stage, since its results are capable of reflecting changes in fuel consumption, GHG emissions and cost for different locations and driving scenarios in order to facilitate the deployment of a sustainable transportation system towards meeting CAFE 2025 targets.

REFERENCES

1. EPA and NHTSA Set Standards to Reduce Greenhouse Gases and Improve Fuel Economy for Model Years 2017-2025 Cars and Light Trucks, 2012. http://www3.epa.gov/otaq/climate/documents/420f12051.pdf
2. Singh, R., Alapatt, G. F. and Abdelhamid, M., "Green energy conversion & storage for solving India's energy problem through innovation in ultra large scale manufacturing and advanced research of solid state devices and systems, "in Proc. Int. Conf. Emerg. Electron, Dec. 15-17, 2012, pp. 1-8.
3. Singh, R., Asif, A. A., Venayagamoorthy, G. K., Lakhtakia, A., Abdelhamid, M., et al., " Emerging role of photovoltaics for sustainably powering underdeveloped, emerging, and developed economies," in Proc. 2nd Int. Conf. Green Energy and Technology (ICGET), IEEE, Sep. 5-6, 2014, pp. 1-8.
4. Abdelhamid, M. "A comprehensive assessment methodology based on life cycle analysis for on-board photovoltaic solar modules in vehicles" , Paper 1458 , 2015 [online] Available: http://tigerprints.clemson.edu/all_dissertations/1458.
5. Mathijsen, D., "Redefining the motor car," Reinf. Plast. 00(00), 2015, doi:10.1016/j.repl.2015.04.011
6. Ford C-MAX Solar Energi Concept, Retrieved March 20, 2015, [Online]https://media.ford.com/content/fordmedia/fna/us/en/news/2014/01/02/let-the-sun-in--ford-c-max-solar-energi-concept-goes-off-the-gri.html
7. Abdelhamid, M., Singh, R., Qattawi, A., Omar, M., and Haque, I., "Evaluation of On-Board Photovoltaic Modules Options for Electric Vehicles," Photovoltaics, IEEE Journal of. 4(6): 1576-1584, 2014.
8. Abdelhamid, M., Qattawi, A., Singh, R., and Haque, I. "Comparison of an Analytical Hierarchy Process and Fuzzy Axiomatic Design for Selecting Appropriate Photovoltaic Modules for Onboard Vehicle Design," International Journal of Modern Engineering, 15(1): 23-35, 2014.
9. Abdelhamid, M., Singh, R., and Haque, I., "Role of PV generated DC power in transport sector: Case study of plug-in EV." In DC Microgrids (ICDCM), 2015 IEEE First International Conference on, pp. 299-304. IEEE, 2015.

10. U.S state solar map SolarGis. [Online]. Available: http://solargis.info/doc/postermaps.
11. González-Longatt, F. M. " Model of photovoltaic module in Matlab™," II CIBELEC, pp. 1-5, 2005.
12. Soto, W. De, Klein, S. A. and Beckman, W. A., "Improvement and validation of a model for photovoltaic array performance," Solar Energy, 80(1): 78-88, 2006.
13. Abdelhamid, M., Singh, R., and Omar, M.," Review of microcrack detection techniques for silicon solar cells," Photovoltaics, IEEE Journal of, 4(1): 514-524, 2014.
14. Tariq, M., Abdelhamid, M., Li, Y., Omar, M., and Zhou, Y., "Fusion of Thermal and Visible Acquisitions for Evaluating Production-borne Scratches and Shunts in Photo-Voltaic PV Cells," Journal of Materials Science Research, 1(4):57, 2012.
15. Sunpower E20/327 Solar Panel. (2014, May 20). [Online]. Avaliable:http://www.rectifier.co.za/Solar/sunpower/pdf/DATASHEET%20-%20SPR-327NE-WHT-D%20FOR%20NORTH%20AMERICA.pdf
16. Hussein, K. H., Muta, I., Hoshino, T., and Osakada, M., "Maximum photovoltaic power tracking: an algorithm for rapidly changing atmospheric conditions, IEE Proceedings-Generation, Transmission and Distribution, 142(1):59-64, 1995.
17. King, D. L., Boyson, W. E., and Kratochvill, J. A., (2004), Photovoltaic Array Performance Model, SANDIA National Laboratories, [Online] http://prod.sandia.gov/techlib/access-control.cgi/2004/043535.pdf
18. National Solar Radiation Data Base, Typical Meteorological Year 3, http://rredc.nrel.gov/solar/old_data/nsrdb/1991-2005/tmy3/by_state_and_city_old.html
19. Alzuwayer, B., Abdelhamid, M., Pisu, P., Giovenco, and Venhovens, P., (2014), Modeling and Simulation of a Series Hybrid CNG Vehicle, *SAE Int. J. Alt. Power,* 3(1):20-29, doi:10.4271/2014-01-1802.
20. Gibson, T. L., and Kelly, N. A., "Solar photovoltaic charging of lithium-ion batteries, Journal of Power Sources, 195(12):3928-3932, 2010.
21. National Household Travel Survey (NHTS). U.S. Dep. Of Transportation Federal Highway Administration, [Online]. Available: http://nhts.ornl.gov/2009/pub/stt.pdf
22. Rizzo, G., Sorrentino, M., and Arsie, I., "Rule-Based Optimization of Intermittent ICE Scheduling on a Hybrid Solar Vehicle," *SAE Int. J. Engines* 2(2):521-529, 2010, doi:10.4271/2009-24-0067.
23. U.S DOE, fuel economy http://fueleconomy.gov/
24. PVinsights Grid the World. (2014, Oct. 1). [Online]. Available: http://pvinsights.com/index.php
25. Analytical Modeling Linking FASTSim and ADOPT Software Tools. [Online]. Available: http://energy.gov/sites/prod/files/2014/03/f13/van004_brooker_2013_o.pdf
26. Miller, J. Energy Storage and Battery Advances. [Online]. Available: http://www.eei.org/about/meetings/Meeting_Documents/Miller,%20James.pdf
27. GREET Model, Argonne Lab, [Online] http://greet.es.anl.gov/.
28. Lenner, M. Influence of roof-rack, trailer etc on automobile fuel consumption and exhaust emissions, measured on-the-road. SAE Technical Paper 1998; No. 980682
29. Thomas, J., Huff, S., and West, B., "Fuel Economy and Emissions Effects of Low Tire Pressure, Open Windows, Roof Top and Hitch-Mounted Cargo, and Trailer," *SAE Int. J. Passeng. Cars - Mech. Syst.* 7(2):862-872, 2014, doi:10.4271/2014-01-1614.
30. Brooker, A., Ward, J., and Wang, L., "Lightweighting Impacts on Fuel Economy, Cost, and Component Losses," SAE Technical Paper 2013-01-0381, 2013, doi:10.4271/2013-01-0381

CONTACT INFORMATION

Dr. Mahmoud Abdelhamid
mabdelh@g.clemson.edu

mabdelhamid@ucmerced.edu

DEFINITIONS/ABBREVIATIONS/ NOMENCLATURE

Mono-Si - mono-crystalline silicon

PV cell - Photovoltaic solar cell

ICE Vehicle - Internal combustion engine powered vehicle

CAFE - Corporate Average Fuel Economy

Rs - Series resistance

I - $_d$ Shockley diode current

I_{PV} - Incident light

I_{SC} - Short circuit current

V_{oc} - Open circuit voltage

R_p - Parallel resistance

n - Diode ideally factor

q - Electron charge

k - Boltzmann constant

G - Global solar irradiation

G(nom) - Nominal solar irradiation (1000 W/m^2)

T_1 - Reference temperature 25°C)

T_2 - Arbitrary temperature

$I_{SC}(T)$ - Short circuit current at specific temperature

T - Cell temperature

I_0 - Reverse saturation current

C_d - Aerodynamic drag

ρ_a - Density of air

DHI - Diffuse horizontal irradiance

DNI - Direct normal irradiance

A_f - Frontal projected area

C_r - Rolling resistance

v - Vehicle velocity

MPG - Mile per gallon

STC - Standard test conditions: solar irradiance of 1000 W/m^2, AM 1.5, and cell temperature 25 °C

ROI - Return on Investment

η_{T2W} - Tank to wheel efficiency

APPENDIX

Table 1. Total energy stored in battery by proposed PV module system

Scenario	Hourly 9-10 am	Hourly 12-1pm	Hourly 4-5 pm	Daily
Minimum Scenario: Boston, MA (December)	73 Wh	187 Wh	31 Wh	1.036 kWh
Maximum Scenario: Phoenix, AZ (June)	441 Wh	572 Wh	317 Wh	4.81 kWh

Table 2. Total cost of investment for entire hybrid solar powertrain components

Component	Quantity	Current Price ($)	Future Price ($)	Note
PV Module	654 W	616	350	Current PV module price with no tax $0.88/W [24] for future price $0.50/W (DOE target). Adding 7% Tax
Battery	5 kWh	2525	1525	125 $/kWh by 2022 Equation (24)
Motor and controller	10 kW	642	642	Equation (23)
Total		3,783	2,517	

Table 3. Weight analysis by PV added on-board to gasoline vehicle

Component	Quantity	Weight (kg)	Note
PV Module	3.26 m^2	37.0	17.58 W/kg [7]
Mounting	1 unit	4.0	Assumed
Battery	5 kWh	83-100	83 kg based on specification 60 Wh/kg [19]. 100 kg based on Equation (27)
Electric motor	10 kW	11.0	Based on [30]
Total (Add weight)		+135 to 152	
Remove weight from the engine	10 kW	-5.0	Equation (26)
Powertrain weight will increase by		~ Extra 130.0 to 147 kg	